Lasing features in scattering gain media and amplified spontaneous emission systems

ARTICLE *in* JOURNAL OF APPLIED PHYSICS · JULY 2006

Impact Factor: 2.18 · DOI: 10.1063/1.2218030

Lasing features in scattering gain media and amplified spontaneous emission systems

M. A. F. de Souza and A. Lencina
Departamento de Física, Centro de Ciências Exatas e da Natureza, Universidade Federal da Paraíba, Caixa Postal 5008, João Pessoa, Paraíba 58051-970, Brazil

P. Vaveliuk[a)]
Departamento de Física, Universidade Estadual de Feira de Santana, Campus Universitário, BR 116, Km 03, Feira de Santana, Bahia 44031-460, Brazil

(Received 14 September 2005; accepted 19 May 2006; published online 25 July 2006)

An experimental study was made on lasing features in both scattering gain media and amplified spontaneous emission systems from a rhodamine-6G xanthene dye in ethanol solution. The emission intensity, spectral line-half-width, and lasing threshold are investigated in terms of dye concentration, cell thickness, and pump energy. The analysis shows that both systems behave quite different. It was found that the scattering gain media present best lasing properties which are enhanced to smaller cell thickness where the backscattering effect plays a significant role. In addition, its laserlike characteristics were found slightly dependent on dye concentration within the range in which the dimer species influence is absent. In return, the amplified spontaneous emission systems were observed strongly dependent on the product of cell thickness and dye concentration, namely, optical density. These systems present lasing properties only around an optimized value of optical density. Within this range, their emission intensity, spectral line-half-width, and threshold could overcome those obtained from scattering gain media. © *2006 American Institute of Physics*. [DOI: 10.1063/1.2218030]

I. INTRODUCTION

Lasing action without external cavity was found in several physical systems as, for example, xanthene dye solutions. At adequate pump laser excitation and gain volume, a simple solution of organic dye could behave as an amplified spontaneous emission (ASE) system.[1] The ASE consists of laserlike emission from a high gain medium with a single pass of pump radiation. The light amplification is due to the molecular planes of the active medium resonating coherently even without a presence of an external cavity.[2] The ASE influence is crucial when the dye gain characteristics in amplification systems with oscillator are studied because the ASE has a different wavelength and spectral line-half-width than that produced by conventional laser emission, being able to cause background noise.[3] On the other hand, when an adequate concentration of scatterer nanoparticles is added, the dye solution becomes a colloidal suspension that could also present lasing features.[4] These systems are often called scattering gain media (SGM) and consist of laserlike emission from an active scattering medium, also without cavity, consequence of a light amplification with nonresonant feedback caused by scatterers.[5] The study of this class of systems grew quickly due to their potential applications.[6]

After the observation of a SGM in xanthene dyes,[4] different interpretations about the amplification processes were suggested. For example, Ref. 7 proposes that the effect of the scatters in the experimental setup used in Ref. 4 should only cause scattering of the ASE so that the scatterers do not act as amplifiers and, therefore, the SGM should be interpreted as *diffuse* ASE according to the theoretical model proposed by the work of Letokhov.[8] The divergence was partially removed when the threshold of SGM was found dependent on the scatterer concentration contrary to what happens in diffuse ASE.[9] Thus, the differences between SGM and ASE were deepened with the appearance of bichromatic emission, i.e., two well-defined peaks in the emission spectrum product of the contribution of monomer and dimer aggregates,[10] that was observed exclusively in SGM.[11,12] However, in spite of SGM and ASE systems having been widely studied separately, a simultaneous analysis of their laserlike features in terms of dye concentration, cell thickness, and pump energy has never been carried out. As a consequence, the fundamental similarities and differences of both systems are still not completely known. From the above, the aim of this work is to study the emission intensity, spectral line-half-width, and laser threshold for an ethanol solution of rhodamine-6G with and without nanoparticle scatterers. With this, it should be possible to obtain and compare the principal lasing characteristic of SGM and ASE, determining the parameter range in which both systems present the best and worse performance.

The paper is structured as follows. In Sec. II, we describe the experimental setup. Sec. III presents the main results of the experimental measurements. Section IV discusses the results obtained for ASE and SGM individually as well as comparatively showing the main features of both systems. Finally, in Sec. V, we conclude.

II. THE EXPERIMENTS

The experiments consisted of measuring the emission spectra of the rhodamine-6G chlorate laser dye (Rh-6G) in

[a)]Electronic mail: pablov@fisica.ufpb.br

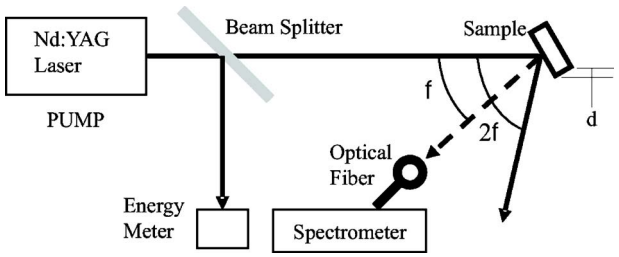

FIG. 1. Schematic diagram of the experimental setup. The cell thickness is symbolized by d. The dye emission was collected at $\phi=15°$.

ethanol-aerated solutions at room temperature (22 °C) with (ASE system) and without scatterers (SGM system); the setup is shown in Fig. 1. The Rh-6G was supplied by Exciton and the ethanol by Merck. Cells of 1.0 and 0.1 cm of depth were used for dye concentrations of 5×10^{-5}, 1×10^{-4}, 5×10^{-4}, and $1\times10^{-3}M$. The scatterer concentration was 10 mg/cm$^3\approx10^{11}$ particles/cm^3. All samples (SGM and ASE) were optically pumped by a frequency doubled and Q-switched Nd:YAG (yttrium aluminum garnet) laser. The pump laser pulse duration was 5 ns, the repetition rate was 10 Hz, and the beam diameter was about 2.4 mm. The data were recorded by using an Ocean Optics fiber optic spectrometer with a resolution of about 0.7 nm. The energy of the pump beam was varied from 0.002 to 18 mJ.

III. RESULTS

In this section we present the main results on the lasing features of ASE and SGM systems for different cell thickness and dye concentration summarized into three tables. Table I gives the ratio of emission intensity between the cells with $d=1.0$ and 0.1 cm for ASE and SGM for the different concentrations. It is observed that the SGM emission intensity is higher for $d=0.1$ cm than that for $d=1$ cm, its ratio being approximately constant regardless of the C value. On the other hand, the ASE emission intensity as well as its ratio strongly depend on C. For low concentrations, the dye solution for $d=1$ cm emits more intensively than for $d=0.1$ cm. The contrary occurs for high concentrations: the dye intensity for $d=0.1$ cm exceeds that for $d=1.0$ cm.

Table II refers to another crucial lasing parameter: spectral line-half-width or also known as full width at half maximum (FWHM). The FWHM of SGM presents negligible variation on the C changes for fixed values of d. The 0.1 cm cell shows a minor FWHM than the 1.0 cm cell. For ASE, the FWHM strongly presents variations for opposite values of the concentration, these changes being different for both cells. For low concentrations, the dye solution within the cell of $d=1$ cm shows a thinner FWHM than that for $d=0.1$ cm. The contrary occurs for high concentrations: the FWHM for $d=0.1$ cm strongly exceeds that for $d=1.0$ cm.

Table III presents the energy threshold E_{th} (Ref. 13) for ASE and SGM. The SGM E_{th} does not depend on C for fixed thickness, being slightly smaller for cells of 0.1 cm. On the other hand, the ASE E_{th} shows strong dependence on those parameters. For low concentrations, the dye solution within the cell of $d=1$ cm shows lasing behavior contrary to what occurs for $d=0.1$ cm. The inverse occurs for high concentrations: threshold exists for $d=0.1$ cm contrary to what happens for $d=1.0$ cm. In some excitation cases, the ASE system could not show laserlike behavior within the pump energy range used in our experiments and, therefore, the E_{th} was not able to be defined. This fact is indicated by the asterisks in the table.

Globally, from Tables I–III, we point out the strong dependence of the ASE on C and d. It will show that a simple combination of them should be used to know the regime where the ASE system could reach better lasing features. On the other hand, for SGM, we observed a negligible dependence on C and their better lasing properties reveal for very thin cell thickness which suggests an efficient backscattering mechanism. For a deeper analysis, we introduce the relevant absorption and scattering scales: the absorption length, estimating the mean path traveled by photons before to be absorbed, defined as $\ell_a=1/N\sigma_a$, being σ_a the absorption cross section at the respective wavelength and N the dye nonexcited molecule density; the scattering mean free path ℓ_s, estimating the average distance between two scattering events, defined by $\ell_s=1/N_s\sigma_s$, being σ_s the scattering cross section

TABLE I. Ratio of emission intensity for ASE and SGM for different concentrations between the samples for cell thickness of 1.0 and 0.1 cm. The pump energy was 18 mJ in all cases.

Dye concentration (M)	$I_{\text{em}}(d=1.0\text{ cm})/I_{\text{em}}(d=0.1\text{ cm})$	
	ASE	SGM
5×10^{-5}	1.4×10^{7}	6.4×10^{-1}
1×10^{-4}	1.4×10^{6}	6.0×10^{-1}
5×10^{-4}	0.9×10^{1}	6.1×10^{-1}
1×10^{-3}	1.7×10^{-3}	6.0×10^{-1}

TABLE II. FWHM at 18 mJ pump energy for ASE and SGM for all cell thickness and concentrations used.

Dye concentration (M)	Spectral line-half-width (nm)			
	$d=1.0$ cm		$d=0.1$ cm	
	ASE	SGM	ASE	SGM
5×10^{-5}	2.4	4.1	33.0	3.0
1×10^{-4}	2.6	4.0	22.1	2.9
5×10^{-4}	2.8	4.3	2.6	3.0
1×10^{-3}	20.7	4.0	3.3	3.1

TABLE III. Threshold energy for ASE and SGM for all cell thickness and concentrations used.

Dye concentration (M)	Lasing energy threshold (mJ)			
	$d=1.0$ cm		$d=0.1$ cm	
	ASE	SGM	ASE	SGM
5×10^{-5}	0.7	0.14	* *	0.11
1×10^{-4}	0.8	0.14	* *	0.10
5×10^{-4}	2.8	0.14	1.0	0.10
1×10^{-3}	* *	0.15	2.1	0.11

and N_s the scatterer particle density, and the transport mean free path ℓ_t, defined as the average distance a wave travels before its direction of propagation is randomized.[15] ℓ_t and ℓ_s are directly related by $\ell_t=\ell_s/(1-\langle\cos\theta\rangle)$, where θ is the averaged-scattering angle, which in a Mie regime takes small values. For the samples with dye concentrations given in Tables I–III: 5×10^{-5}, 1×10^{-4}, 5×10^{-4}, and $1\times10^{-3}M$, $\ell_a\sim833$, 417, 83.3, and 41.7 μm, respectively, for $\sigma_a\sim4.0\times10^{-16}$ cm^2 at $\lambda_p=532$ nm.[16] $N_s\sim10^{11}$ particles/cm^3 corresponds to a transport mean free path $\ell_t\sim35$ μm for pump photons, and $\ell_{te}\sim41$ μm for dye emitted photons ($\lambda_{em}\sim565$ nm). The physical implications of the principal features are discussed in detail in the following section.

IV. DISCUSSION

This section was divided into three parts: the first devoted to analysis of the SGM principal characteristics, the second, to the ASE and the third, to comparatively study both systems.

A. SGM lasing features

Table I emphasizes an invariance of the emission ratio between both thin and thick cuvettes on the dye concentration for these amplifying random media. To explain this constancy, we introduce the relevant length parameters that characterize the amplification region. The critical volume V_{cr} can be defined as the maximum effective amplification volume being $V_{cr}=\phi\times L_{cr}$ with ϕ, the excitation beam spot diameter and L_{cr}, the critical penetration depth that describes the maximum effective amplification length, above which the intensity diverges. The critical thickness can be approximated by $L_{cr}\sim\pi\sqrt{\ell_t\ell_g/3}$,[15] where ℓ_t was already defined and ℓ_g is the gain length. According to the diffusion model $1/\ell_g\sim\ell_{te}/L^2$,[17] being $L\sim\sqrt{\ell_t\ell_a/3}$,[17,18] the penetration depth or diffusive absorption length. For the dye concentrations given in Tables I–III, $L\sim98$, 70, 31, and 22 μm, respectively. Also, $\ell_t\sim35$ μm and $\ell_{te}\sim41$ μm producing $\ell_g\sim237$, 119, 23.7, and 11.9 μm and $L_{cr}\sim165$, 117, 52, and 37 μm, respectively. Thereby, only slight changes are produced in the amplification process (that depends on L_{cr}/ℓ_g) when the dye concentration is varied, justifying the observed constancy in the emission intensity ratio. Table I also shows that the emission intensity is greater for thin cells that for thick ones. This fact is produced by the reinjection of light into the gain region by the back cell surface, i.e., the well-known backscattering effect, already observed in another class of random media as dye polymer sheet[19] and ZnO polycrystalline films.[20] Due to backscattering, the photon traveled mean path and the scattering events within the active medium increase improving the amplification process and, consequently, the laserlike properties. To understand this effect, we analyze the real penetration depth for each dye concentration value. As the L values are lesser than the 0.1 cm cell thickness, the backscattering hypotheses should not be true. However, the experimental conditions were under a saturation regime. In fact, the excitation intensity used in the work, $I_0\sim5.1\times10^{10}$ mW cm^{-2}, was larger than the saturation intensity $I_s\sim2.5\times10^8$ mW cm^{-2} [$I_s=h\nu/\sigma_e\tau$ with σ_e, the emission cross section and τ, the dye excited stated lifetime, with $\tau\sim3.5\times10^{-8}$ s and $\sigma_e\sim3.0\times10^{-16}$ cm^2 (Ref. 16). Thereby, the real penetration depth L_R becomes greater than L and can be estimated by using the energy conservation as $L_R\sim\sqrt{I_0\ell_a\ell_t/I_s}$.[17] For the respective concentrations in tables, the calculus gives $L_R\sim0.29$, 0.21, 0.11, and 0.08 cm. This would be in agreement with the fact that the backscattering occurs for 0.1 cm cell but not for 1.0 cm cell.

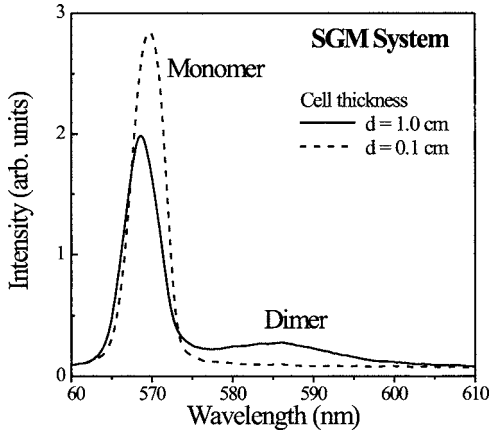

FIG. 2. Emission spectra of SGM at high dye concentration and different cells. The cell of 0.1 cm presents a major intensity and is redshifted. Besides, its spectrum does not present the dimer fluorescence peak. The dye concentration was $1\times10^{-3}M$ and pump energy of 18 mJ.

The backscattering effect is clearly evidenced in Fig. 2 where the emission spectra for both thickness cells are depicted. The laser peak for thin cells is greater than for thick ones. Besides, the maximum for thin cells is slightly redshifted and does not present a secondary fluorescent peak at major wavelengths as it does for thick cells. This peak is generated by another dye aggregate: the dimer species.[10,12] These peculiar spectral differences between both spectra should be attributed to reabsorption processes. It is well known that the spectral shift of emission peaks, often called Stokes shift, is a consequence of the partial overlap between absorption and fluorescence cross sections of singlet monomer species so that the degree of the Stokes shift is determined by the strength of the monomer-monomer reabsorption processes.[12,21] On the other hand, there is a quasicomplete overlap between dimer absorption and monomer fluorescence bands for Rh-6G.[23] As the mean path traveled by the monomer emitted photons is greater for thick cells than for thin ones, the probability of reabsorption by dimers is also greater for thick cells, weakening the monomer-monomer reabsorption process. Thereby, the dimer emission increases in detriment of monomer emission causing an appreciable secondary peak only for thick cells. The lesser monomer-monomer reabsorption probability for thick cells, caused by monomer-dimer reabsorption appearance, explains a major redshift of the principal peak for thin cells. It is important to note that identical Stokes shift occurs between both cell spectra when the dye concentration is increased: the thin cell emission peak is redshifted with respect to the thick one and presents a greater peak strength. The only difference is that a secondary peak also appears for thin cells although always less intense than for thick cells. This

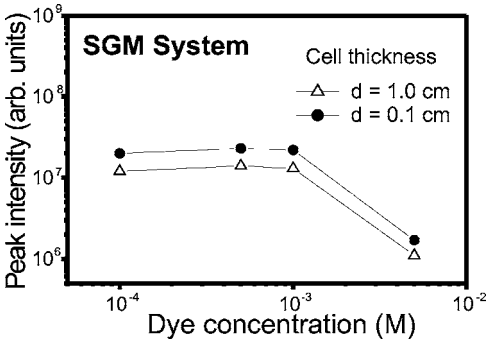

FIG. 3. Maxima of SGM emission intensity against dye concentration for $d=0.1$ and $d=1.0$ cm. Only for high concentrations appears a significant decrease of the maximum of the monomer intensity due to the dimers presence.

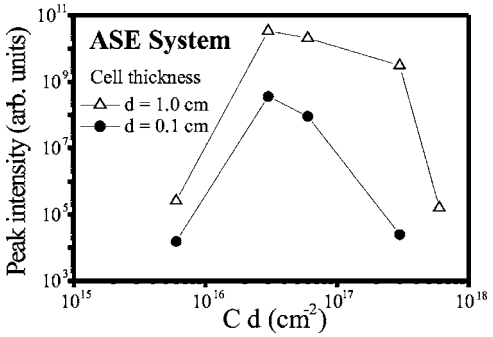

FIG. 5. Influence of the optical density ($D \sim Cd$) in the dye intensity emission to two cells. The pump energy was of 18 mJ.

was observed for emission spectra at $C=5\times10^{-3}M$, which shows that the thin cell does not inhibit the appearance of the secondary peak but it simply retards it. It should be clear that the dimer activity is related to the reabsorption (not backscattering) processes. The peak emission constancy on dye concentration increasing at fixed thickness is visualized in Fig. 3. However, from relatively high concentration values ($\geqslant10^{-3}M$), a peculiar decrease of intensity is produced when C is increased. For these concentrations, the dimer population in thermal equilibrium with the monomers is significant. Therefore, this quenching of peak emission is a consequence of a strong monomer-dimer reabsorption process and posterior dimer reemission at higher wavelengths in accordance with the comments about Fig. 2.

Finally, our results show that the backscattering occurring for thin cells also slightly reduces the FWHM and lasing threshold which is shown in Tables II and III and in Fig. 4. The black solid points correspond to 0.1 cm cell whose sigmoidal curve is hardly below the curve corresponding to 1.0 cm cell values. Therefore, the threshold for thin cells indicated by the arrow (2) is shifted to lower pump energy values. It is shown in Fig. 4 that the points for different concentrations and fixed cell values are strongly superimposed which indicates a negligible dependence of the FWHM and threshold intensity on the dye concentration which is also supported in Tables II and III. This is due to the threshold reached at an intensity value for which the pump transition is bleached.[22] Under this condition and according to Ref. 17, the threshold intensity can be estimated as $I_{\text{th}} \sim I_s \ell_g / \ell_a$. When a constant I_{th} value is reached for a dye concentration increasing, the gain length ℓ_g reaches an absolute minimum (gain maximum). This minimum value can be estimated assuming a complete population inversion by $\ell_g^{(\min)} \sim 1/N_t \sigma_e$, where N_t is the total dye molecule density and σ_e is the excitation cross section. A calculus gives $\ell_g^{(\min)} \sim 1111$, 555.6, 111.1, and 55.6 μm and $\ell_a \sim 833$, 417, 83.3, and 41.7 μm so that the ratio ℓ_g / ℓ_a is practically constant justifying the I_{th} constancy on the dye concentration changes for SGM.

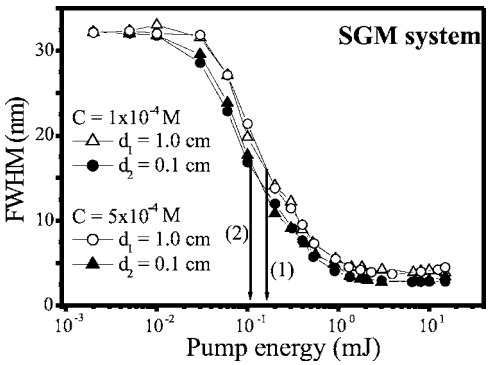

FIG. 4. Spectral line-half-width vs pump energy for several concentrations and cell thickness. The arrow indicates the laser threshold for several d: (1) 1.0 cm and (2) 0.1 cm. Note that the threshold does not depends on C.

B. ASE lasing features

Our experimental results indicate that the ASE strongly depends on both parameters: C and d. This class of systems presents quite different behavior for different range of values of such parameters within the pump energy range used. Table I shows that for thick cells, the major peak emission intensity occurs in lower concentrations, contrary to thin cells where the major emission intensity occurs at higher concentrations. For conventional laser dyes, the emission peak strength strongly depends on the product of cell thickness d and dye concentration C.[24,25] The authors of these references analyzed the emission properties in terms of a parameter that depends on geometrical properties and excitation intensity: the optical density D. At fixed value of pump energy, $D \sim Cd$. They observed that there is a maximum emission intensity for an optimized value of D. Our ASE system behaves similarly as Fig. 5 shows. The correlation of D with the lasing properties is supported by Tables II and III. The amplification process of the neat dye ASE system that only depends on gain coefficient and penetration length happens when the excitation intensity is sufficiently large to produce inversion of the population and saturation in the amplification region, which, we believe, only occur for optimized values of D. Otherwise, if this condition is not reached, the system presents an emission with character fluorescent or a mixed fluorescence lasing, as the inset of Fig. 6 shows. Thereby, D is crucially important since it gives a qualitative form to analyze the fluorescence and lasing situations of neat dye ASE systems. We observe that the optimized D value implies certain combinations between C and d: small ℓ_a (high dye concentration) needs small d values and high ℓ_a

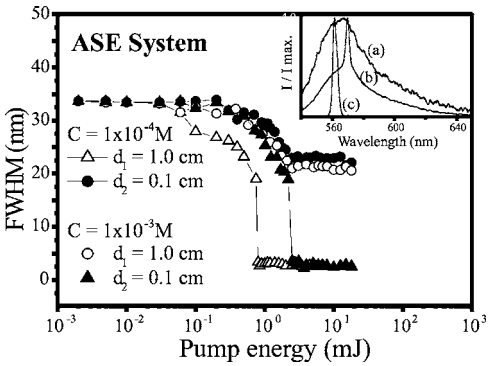

FIG. 6. Spectral line-half-width vs pump energy for several concentrations and cell thickness. The inset shows the emission spectra for ASE at different pump energies: (a) 0.1 mJ, fluorescence, (b) 1.5 mJ, mix, and (c) 3.3 mJ, laserlike. The concentration was $1\times10^{-3}M$ and $d=0.1$ cm.

(small dye concentrations), greater d values. Thereby, the changes in the emission intensity should be prominent from 0.1 to 1.0 cm for the different concentrations and the transition fluorescence lasing happens in opposite ways for the two cells in relation to the dye concentration variations as Tables I–III show.

In addition, two aspects should be clarified from Fig. 5. The cell of 1.0 cm presents a major peak intensity for D fixed values. It can be explained by the fact that the gain is proportional to the excited volume in ASE systems (as in conventional dye lasers) such that for $d=1.0$ cm it is greater than that for $d=0.1$ cm. The absorption length, calculated in Sec. III, is smaller than the cell thickness and consequently, the parameter d should not be important. However, as the experiments were performed under saturation regime, the real penetration depth L_R becomes larger than ℓ_a being able to be estimated as $L_R\sim\sqrt[3]{I_p\ell_a\phi/I_s}$.[17] From the excitation intensity for all dye concentrations used in the tables, the values estimated of L_R are 1.6, 1.3, 0.8, and 0.6 cm. These values are not much lesser than cell thickness and support the importance of this parameter. Another peculiar feature is the decrease of the ASE emission when the dye concentration increases. It can be explained as follows: ASE presents different transverse and longitudinal emissions with respect to the pump beam. For Rh-6G, both emissions were observed, for example, in Ref. 26. It was pointed out earlier that there is competition of both modes and, for high dye concentrations, the transverse mode becomes dominant due to the scattering of light from the nonhomogeneous heat distribution that the pump beam generates, prejudicing thus the longitudinal emission.[25] In addition, we believe that the strong monomer-dimer reabsorption process contributes to the reduction of principal peak emission.

On the other hand, Tables II and III show that for thick cells, the minor FWHM and threshold occur at lower concentrations, while for thin cells, the major FWHM and threshold occur at higher concentrations which support that lasing action occurs for optimized D value and also gives a qualitative form to analyze both fluorescence and lasing situations of neat dye ASE systems. For certain ranges of C and d, the ASE does not present laserlike behavior: either for thin cells and lower concentrations or for thick cells and higher concentrations. These facts are shown in Fig. 6: FWHM versus pump energy for both cells and varying concentrations. Note that for optimized values of Cd, the fluorescence-laserlike transition occurs in the form of a step while that for nonoptimized values, the transition is inhibited.

In summary, the above suggests that, for fixed pump energy, a single parameter, either C or d, would not be sufficient to study the fundamental characteristics of such class of systems. Thereby, the optimized lasing characteristics could be given for an optimized combination of both parameters. This was not pointed out in the past in the papers devoted to study the ASE behavior.

C. ASE versus SGM

Here, we discuss the main differences between both systems. It is important to note that the essential differences are only pointed out when a simultaneous analysis is performed in terms of the cell thickness, dye concentration, and, in addition to, the pump energy. The fact that the SGM could or could not be equivalents to diffuse ASE systems was analyzed in terms of the role played by the scatterers.[4,7] The controversy in these papers was perhaps originated by the fact that both groups performed the experiments at high dye concentrations but different excitation setups. In Ref. 4 the emission intensity was detected longitudinally while that in Ref. 7 it was detected transversally. It is possible that the strong dependence of the ASE emission properties on this factor was not taken into account in these works.

It is a well-known fact that the effect of the scatterers in the emission properties of a dye solution is critical.[11] The ASE is a relevant phenomenon for an excited neat dye solution for an optimized set of values of optical density. However, their laserlike emissions could be quenched when a small amount of scatterers is added, appearing as fluorescent emission only. Thus, laserlike emission appears again for certain scatterer concentration that optimizes the mean free path of the photons to get a light amplification process.[18] Another aspect demonstrating the crucial scatterer influence in a dye solution is that SGM is able to generate laser action even at very small gains (low dye concentration and thin cuvette, see Table III) which would never happen for an ASE system.

Both types of systems present marked differences in their threshold and FHWM properties. The FWHM spectral emission variation rate essentially depends on the amplification process which is different in both systems: neat dye solution and dye solution with optimized scatterer density. For the latter, nonresonant feedback of diffusive photons inside of the gain media is the cause of the gain narrowing process. This fact implicates that the whole fluorescence spectral range is amplified simultaneously. Therefore, the FWHM variation produces smoothly as observed in Fig. 4. Compared with SGM system, a minor fluorescence spectral range is amplified to produce lasing action in a neat dye ASE system. As a consequence, the fluorescence-lasing transition occurs abruptly (Fig. 6), as well as it happens in the conventional laser. This different transition for both systems also brings different energy threshold behavior. It is well known

that a fundamental trait of SGM is their very low threshold which turns it into a very efficient laserlike system.[4] However, our results show that the *effective* ASE threshold could overcome the SGM one in certain conditions. This fact was not pointed out in the past. As the SGM fluorescence-laserlike pump energy transition region is relatively wide and its threshold is given by the inflection point of a sigmoidal fit,[13] this value could be situated at much lower energy than the effective energy for which the laserlike emission characteristics appear. It can be observed in Fig. 4 that $E_{\text{th}}(\text{SGM}) \approx 0.2$ mJ for $d=1.0$ cm while the effective energy value, where the laser emission rises, is $E_{\text{eff}}(\text{SGM}) \approx 1.0$ mJ. On the other hand, the ASE presents approximately a step transition rather than sigmoidal for optimized D values. Then, necessarily in this case $E_{\text{th}}(\text{ASE}) \equiv E_{\text{eff}}(\text{ASE})$. Note that $E_{\text{eff}}(\text{ASE}) < E_{\text{eff}}(\text{SGM})$. For example, in Fig. 6, for $C = 10^{-4}M$ and $d=1.0$ cm, $E_{\text{eff}}(\text{ASE}) \approx 0.8$ mJ major than 0.2 of $E_{\text{th}}(\text{SGM})$ of Fig. 4. However, the threshold features of ASE are better results than that of SGM when the effective values, 0.8 and 1.0 mJ, respectively, are compared. These threshold and FWHM behaviors should be extended for any sample that behaves as either ASE or SGM.

Also, another peculiar behavior can be remarked from Table II: the FWHM in SGM is larger than in ASE for thick cell (4.1 nm vs 2.6 nm) in spite of the linewidth of ASE which should be broad under saturation condition. This can be explained as follows. The absorption and emission bands of organic dyes in solution are inhomogeneously broadened because of the solvent-solute interaction. In a typical ASE process, the line-half-width of spontaneous emission could narrow around 15 times. When saturation effects are taken into account in inhomogeneous broadened media, this narrowing can be significantly reduced, especially at higher gain, because their profile saturates first in the center, and thus more gradually in the wings.[2] However, in spite of our system to present a saturated intensity behavior, the normal FWHM broadening process is not observed. The broadening lack in the absorption spectrum was observed in rhodamine-101 (640) ethanol solution under saturation conditions,[27] where a statistical model that includes the solvent interaction effect is proposed. According to this model, the inhomogeneous broadening is caused by the stochastic interaction of the solvent molecules with the dye molecule that forces the system to evolve through a series of configurational states. The presence of a high radiation field generates a steady state molecular distribution of the configurational states. Changing the field fluence, the steady state equilibrium, and so then the spectral response of the medium, changes. By the fact that the rhodamine-6G molecule presents equivalent structural base with the rhodamine-101, we believe that Rh-6G did not present broadening in the saturation regime.

Finally, we remark that our experiments were already performed for an optimized set of values of scatterer concentration. In this context, the crucial parameters characterizing the lasing properties of SGM and ASE are quite different. The product Cd is determinant in the laser features of an ASE system. Only for optimized values of that parameter its lasing properties appear. In return, for the SGM case, the parameter D is not essential for their lasing properties, due to this present negligible dependence on the dye concentration being the cell thickness that introduces changes in their laserlike properties. The best lasing properties in the system SGM reveal optimized values of the product $\ell_t \ell_a$. This association had already been made in Ref. 18. In summary, we state that, in general, the SGM lasing properties are better than those for ASE. However, the latter turns out a very efficient laserlike system for optimized values of the optical density being able to overcome the SGM one. Otherwise, outside of this limit, the ASE either never or weakly becomes laser system.

V. CONCLUSIONS

The lasing features of scattering gain media and amplified spontaneous emission systems raised from a Rh-6G ethanol solution were experimentally studied as function of dye concentration, cell thickness, and pump energy. The analysis shows that both systems could present quite different laserlike features. The laser features of scattering gain media were found slightly dependent on the dye concentration range where the dimer influence is negligible. Their laser properties were found dependent on the cell thickness being enhanced to smaller values where the light backscattering plays an important role. In return, the amplified spontaneous emission was observed to be strongly dependent on the product of dye concentration and cell thickness. It was found that the ASE turns out a very efficient laserlike system for optimized values of the optical density, being able to overcome the SGM lasing properties. Outside this region, their lasing features were either poor or nonexistent.

ACKNOWLEDGMENTS

The authors thank Victor Waveluk for valuable advice. One of the authors (A.L.) was financially supported by CLAF-CNPq and another author (M.A.F.S.) by a PIBIC-CNPq fellowship.

[1] K. Takehisa, H. Nishimura, and A. Miki, J. Appl. Phys. **71**, 1109 (1992).
[2] E. Siegman, *Laser* (University Science Books, Mill Valley, CA, 1986), pp. 547–556.
[3] N. Chi-Kung and A. H. Kung, Rev. Sci. Instrum. **71**, 3309 (2000).
[4] N. M. Lawandy, R. M. Balachandran, A. S. L. Gomes, and E. Sauvain, Nature (London) **368**, 436 (1994).
[5] H. Cao, Waves Random Media **13**, R1 (2003).
[6] N. M. Lawandy, Photonics Spectra **28**, 119 (1994).
[7] D. S. Wiersma, M. P. van Albada, and Ad. Lagendijk, Nature (London) **373**, 203 (1995).
[8] V. S. Letokhov, Sov. Phys. JETP **26**, 835 (1968).
[9] R. M. Balachandran, N. M. Lawandy, and J. A. Moon, Opt. Lett. **22**, 319 (1997).
[10] P. Vaveliuk, A. M. de Brito Silva, and P. C. de Oliveira, Phys. Rev. A **68**, 013805 (2003).
[11] W. L. Sha, C.-H. Liu, F. Liu, and R. R. Alfano, Opt. Lett. **21**, 1277 (1996).
[12] M. A. F. de Souza, A. Lencina, and P. Vaveliuk, Opt. Lett. **31**, 1244 (2006).
[13] The laser threshold can be defined from the changes of FWHM against pump energy as the inflection point of a sigmoidal fit through the data points (Ref. 14). However, this fit cannot be used for the ASE FWHM because it presents a step-type transition.
[14] G. van Soest, M. Tomita, and A. Lagendijk, Opt. Lett. **24**, 306 (1999).
[15] D. S. Wiersma and Ad. Lagendijk, Phys. Rev. E **54**, 4256 (1996).
[16] R. H. Peter, IEEE J. Quantum Electron. **QE-16**, 1157 (1980).
[17] A. L. Burin, H. Cao, and M. A. Ratner, Physica B **338**, 212 (2003).
[18] G. Beckering, S. J. Zilker, and D. Haarer, Opt. Lett. **22**, 1427 (1997).

[19]P. C. de Oliveira, J. A. McGreevy, and N. M. Lawandy, Opt. Lett. **21**, 1685 (1996).
[20]H. Cao, Y. G. Zhao, X. Liu, E. W. Seeling, and R. P. H. Chang, Appl. Phys. Lett. **75**, 1213 (1999).
[21]C. V. Shank, Rev. Mod. Phys. **47**, 649 (1975).
[22]M. Siddique, R. R. Alfano, G. A. Berger, M. Kempe, and A. Z. Genack, Opt. Lett. **21**, 450 (1996).
[23]P. Bojarski, A. Matczuk, C. Bojarski, A. Kawski, B. Kuklinsli, G. Zurkowska, and H. Diehl, Chem. Phys. **210**, 485 (1996).
[24]N. M. Narovlyanskaya and E. A. Tikhonov, Sov. J. Quantum Electron. **8**, 173 (1978).
[25]I. L. Gandel'man, M. V. Melishchuk, and E. A. Tikhonov, Sov. J. Quantum Electron. **13**, 817 (1983).
[26]M. Milano and L. Ferraro, Proc. SPIE **4628**, 22 (2002).
[27]A. O. Marcano, N. Melikechi, and G. Verde, J. Chem. Phys. **113**, 5830 (2000).